



**HAL**  
open science

## From polymer films to organic particles suspensions by means of excimer laser ablation in water

I. Elaboudi, Sylvain Lazare, Colette Belin, David Talaga, Christine Labrugère

### ► To cite this version:

I. Elaboudi, Sylvain Lazare, Colette Belin, David Talaga, Christine Labrugère. From polymer films to organic particles suspensions by means of excimer laser ablation in water. Applied physics. A, Materials science & processing, 2008, 93 (4), pp.827-831. 10.1007/s00339-008-4746-1 . hal-00626933

**HAL Id: hal-00626933**

**<https://hal.science/hal-00626933>**

Submitted on 19 Feb 2024

**HAL** is a multi-disciplinary open access archive for the deposit and dissemination of scientific research documents, whether they are published or not. The documents may come from teaching and research institutions in France or abroad, or from public or private research centers.

L'archive ouverte pluridisciplinaire **HAL**, est destinée au dépôt et à la diffusion de documents scientifiques de niveau recherche, publiés ou non, émanant des établissements d'enseignement et de recherche français ou étrangers, des laboratoires publics ou privés.

# From polymer films to organic nanoparticles suspensions by means of excimer laser ablation in water

I. Elaboudi · S. Lazare · C. Belin · D. Talaga · C. Labrugère

**Abstract** This study highlights the preparation of organic nanoparticles (NP) by laser ablation (LA) of polymeric materials in water. Experiments focused on poly(ethylene terephthalate) (PET) were carried out with the KrF laser pulse (248 nm). Size distribution and concentration of nanoparticles were deduced from suspensions turbidity measurements with the aid of Mie model, by Atomic Force Microscopy (AFM) on the basis of a statistical study and Scanning Electron Microscopy (SEM). The obtained results show that assemblies of spherical NP with a mean diameter 50 nm were synthesised. Composition and surface chemistry of NP were investigated using the Confocal Micro-Raman Spectroscopy (CMRS) and X-ray Photoelectron Spectroscopy (XPS). It indicates that NP are graphitic carbon rich and have a polymeric structure like polyacetylene. The possible mechanisms responsible of NP synthesis by under water LA of polymers was briefly discussed by investigating other polymers targets.

**PACS** 79.20.Ds · 78.67.Bf · 82.70.-y

---

I. Elaboudi (✉) · S. Lazare · C. Belin · D. Talaga  
Institut des Sciences Moléculaires, UMR 5255 du CNRS,  
Université de Bordeaux 1, 351 Cours de la Libération,  
33405 Talence Cedex, France  
e-mail: [i.elaboudi@ism.u-bordeaux1.fr](mailto:i.elaboudi@ism.u-bordeaux1.fr)

C. Labrugère  
Centre de Caractérisation des Matériaux, Institut de Chimie de la  
Matière Condensée de Bordeaux, 87, avenue Albert Schweitzer,  
33608 Pessac Cedex, France

## 1 Introduction

Laser ablation (LA) in liquids presents a unique and fast method to synthesise nanosized objects [1–3] such as nanoparticles (NP), nanowires and nanotubes directly in suspensions that can be further studied, used or processed into a final material whose functionality requires the presence of the new nanostructure. Many synthetic strategies have been developed in recent years to produce and study numerous elemental or compound NP due to their high potential of application in industry (nanotechnologies), in medicine (diagnostics, imaging and treatment of cancer [4], for instance), in biology (immunolabeling, sensing [5–7]), and in research (material, electronics, atmosphere, spectroscopy, catalysis, toxicology [8], microscopies. . .). It is a promising technique for the controlled fabrication of nanomaterials via rapid quenching of ablated species at the interface between solid target and liquid. Numerous studies were focused on synthesis of diamond NP [1], elemental metals (Ag, Au) [9–11] alloys and oxides [12–14] NP. However, little work has been devoted to prepare organic NP by means of laser ablation in liquids. It is, therefore, the purpose of this work to systematically investigate ablation in water of polymeric targets studied for a long time in our laboratory [15] and for which a significant amount of data on ablation in air is available for comparison. In our previous papers, we brought the first evidence of the NP formation by underwater excimer laser ablation of PET and PC [16, 17] by studying the suspension properties as a function of ablation dose (number of pulses). In this paper, we provide additional results more concerned with the chemical composition of NP. An ultimate goal of this work, not yet achieved, would be to provide enough understanding to pre-design a polymeric target for the synthesis of specific NP with predictable properties.

In this framework a number of careful experiment controls (see experimental part) has been setup in order to have a quantitative evaluation of LA efficiency in water: amount of ablated polymer, suspension concentration. These considerations are usually overlooked in recent reports of NP laser ablation of elemental target but necessary for complex multi-element polymeric targets as well as concerns of the chemical modifications of the ablated surface. Interpretations of UV–VIS spectroscopic results, with approximated MIE theory [18], an appealing approach to probe the “as prepared suspension”, are often puzzled by complications due to size-distribution and to aggregation of NP in water which do not allow direct quantification. Other analytical tools (see below) require the deposition of NP on a substrate by drop drying and may lose some of properties of native isolated NP produced in water by the laser pulse.

A set of polymers poly(ethylene terephthalate) (PET), poly(ethylene naphthalate) (PEN), polyimide (PI), poly(methyl methacrylate) (PMMA) and polystyrene (PS) (see below) is studied and the mechanisms involved in the laser ablation are briefly discussed in this paper.

## 2 Experimental

The used polymers are poly(ethylene terephthalate) (PET, Mylar D 75  $\mu\text{m}$ ), poly(ethylene naphthalate) (PEN, Teonex), polyimide (PI, Kapton), poly(methyl methacrylate) (PMMA), and polystyrene (PS).

NP suspensions preparation: The KrF excimer laser irradiation setup giving a square homogeneous spot is described in detail in the recent publications [16]. Samples were immersed inside a spectroscopy type quartz cell which is filled with  $\sim 3$  ml of ultrapure water (Milli Q).

NP investigation: Suspensions can be measured quickly and directly by UV–VIS attenuation spectrometry performed on a Hitachi Model-3200. MIE type interpretation was done with our home-made program (Mathcad) called Mathmie using approximated parameters like index of refraction, density, size, and shape of particles. Other techniques require the deposition of NP on a substrate. It is done by spin coating at 1000 rpm on mica for Atomic Force Microscopy (AFM) just before analysis with a Thermomicroscope CP Research system using intermittent contact mode. Scanning Electron Microscopy (SEM) analysis of NP was done using a JEOL JSM-840 scanning microscope. Samples were also prepared by the same method used for AFM (spin coating) analysis but supported on HOPG (high oriented pyrolytic graphite) substrate. To investigate chemical composition of NP by confocal micro-Raman spectroscopy (CMRS, Jobin Yvon Labram spectrometer equipped with Ar ion laser at 514.3 nm), a layer of particles was prepared on glass substrate by drying a drop of suspension. For X-ray Photoelectron Spectroscopy (XPS) analysis (VG spectrometer

ESCALAB 220-XL, AlK $\alpha$  (1486 eV) some suspension was dropped onto the clean surface of indium. The photoelectron spectrum was done at constant pass energy of 20 eV. The peaks were fitted using a symmetric Lorentzian/Gaussian mixed function (L/G: 25–35%) with the aid of VG Scientific software. In a blank analysis, a drop of ultrapure water was also investigated after being dried in the same conditions to take into account water impurities and indium pollution.

## 3 Results

In our previous study [16], we demonstrated NP formation by LA of PET Mylar D and PC in water. The effect of number of pulses on particle size distribution (PSD) was studied and tendency of NPs to aggregation was concluded due to the increase of NP concentration with ablation dose. Figure 1 shows SEM image of NP prepared from PET Mylar D by LA at 500  $\text{mJ}/\text{cm}^2$  and 100 pulses. We believe it is the evidence of such aggregates of NP. The mean size of these NP is  $\sim 50$  nm as judged in the Fig. 1. This result can be compared to the AFM analysis [17] which was further used to measure the size distribution and indicated the presence of very small particles  $\sim 1$  nm in diameter [16]. These could not be looked for by SEM because of focussing adjustment which is much more time consuming. In addition, analysis of dielectric NP could reduce the resolution (from 1 to 30 nm) of SEM technique due to the accumulation of charges on NP surfaces.

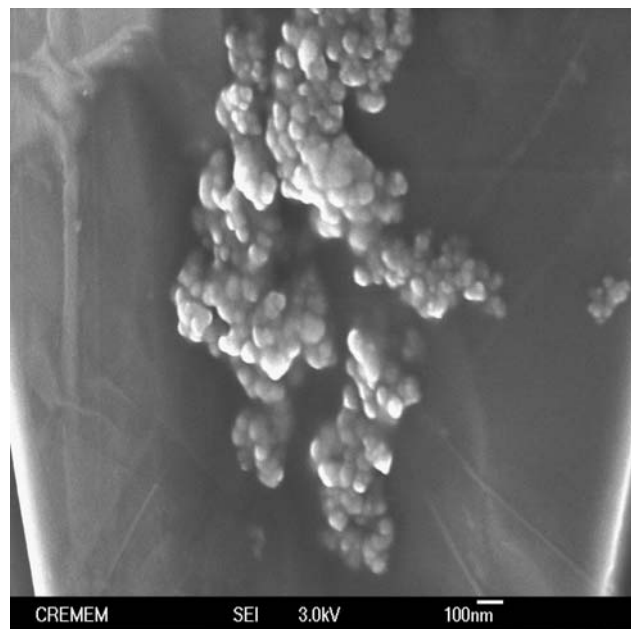


**Fig. 1** SEM image of organic NP prepared by laser ablation of PET Mylar D in water at fluence 500  $\text{mJ}/\text{cm}^2$  and 100 pulses delivered at 1 Hz

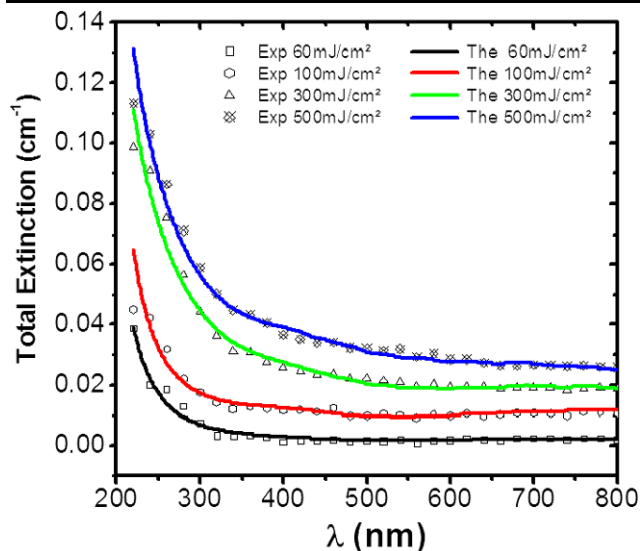


**Fig. 2** Extinction spectra of the aqueous suspensions obtained by laser ablation of PET Mylar D at different fluences. 100 pulses delivered at 1 Hz. (Exp): experimental UV-Vis spectra (*dotted lines*), (The): theoretical spectra calculated using Mie Model (*solid lines*). Reference extinction spectrum of ultrapure water is zero

In order to check whether fluence is an important parameter influencing NP formation, LA with the KrF excimer laser (248 nm) was performed on PET Mylar D at various fluences. NP hydrosols were prepared with 60, 100, 200, 300, and 500 mJ/cm<sup>2</sup> and at fixed number of pulses (100). Figure 2 presents UV-Vis spectra of the obtained suspensions. It shows that eightfold increase of fluence induces fivefold increase of suspension extinction at 248 nm. Therefore, it is possible that NP attenuate the laser fluence (20% is absorbed and scattered after 500 mJ/cm<sup>2</sup> and 100 pulses irradiation) before arriving at the target surface and leads to LA efficiency decrease (by reducing the etching depth) at high fluences. Growth of both size and density of populations of particles explain the increase of suspension extinction with fluence. Approximated Mie theory can be used to support further conclusions by simulations as shown in Fig. 2. To calculate extinction coefficients of suspensions, optical properties of NP were needed; thus, they can be approximated to those of PET Mylar D on one hand (see [16]). On the other hand, Raman spectra show carbon and polymer like NP formation (see below); therefore, the optical characteristics of carbonaceous NP [19] can be considered like in Fig. 2. The calculation procedure of extinction and scattering coefficients was already described in [17, 18] where the shape of NP and some aggregates of NP are assumed to be spherical (as an approximation). A high extinction at shorter wavelengths can be interpreted according to Mie theory as a high density of small particles. Because neither PET nor NP are strong absorbers outside the UV region [19, 20], a high extinction at longer wavelengths is attributed to scattering of a high density of larger particles essentially.

**Table 1** Particle size distributions (PSD) and density of NP used in the approximated Mie model to fit UV-Vis spectra in Fig. 2

Fluence (mJ/cm <sup>2</sup> )	Diameter (nm)	Density (particles/cm <sup>3</sup> )
60	40	$2 \times 10^{11}$
	1200	$5 \times 10^6$
100	40	$4 \times 10^{10}$
	460	$6 \times 10^7$
300	1200	$2 \times 10^7$
	80	$9 \times 10^{10}$
	520	$1 \times 10^8$
500	1200	$3 \times 10^7$
	80	$1 \times 10^{11}$
	520	$2.5 \times 10^8$
	1200	$3.5 \times 10^7$

Table 1 shows results of simulation indicating the possible formation of new populations of NP with larger size (80 nm, 1200 nm) and disappearance of population of NP with small size (40 nm). This behaviour could be explained by the aggregation phenomenon which is strongly favoured at high concentration of particles produced by large dose of LA.

Numerous experiments on LA of PET Mylar D were done in air and vacuum in past studies. Gaseous and solid products of ablation were already investigated and interpreted with photochemical and photo-thermal effects which are the main ablation mechanisms at the KrF laser wavelength (248 nm) [15]. In these conditions product collection mode is limited to deposition on surface an approach which only allows aggregates, whereas “in water ablation” allows preparation of more dispersed single NP that could be addressed individually for analysis or used further. NP were characterised by CMRS and XPS, two spectroscopies that are sensitive to nm thick particles of matter. XPS (Fig. 3) allows identification of elemental composition whereas CMRS mainly described previously [16] identifies bond vibrations. With XPS, the depth of analysis is given by the elastic photoelectron mean free path and is about 50 Å. Figure 3 presents two sets of ablation condition (B) low fluence at 23 mJ/cm<sup>2</sup>, 900 pulses and high fluence (C) at 640 mJ/cm<sup>2</sup>, 40 pulses. The first fluence is lower than the ablation threshold of PET Mylar D in air ( $Ft = 30$  mJ/cm<sup>2</sup>); however, formation of NP was indeed observed and independent recent study of laser kinetic ablation made underwater confirmed the reduction of the ablation threshold of PET ( $\approx 14$  mJ/cm<sup>2</sup>) [21] by doing it in water. This effect will be presented in an upcoming paper.

NP and other particles investigated by CMRS are completely different from that of starting PET film. In the Raman spectra of some products obtained at high fluence (640 mJ/cm<sup>2</sup>, 100 pulses), display bands attributed to C=C, C-C, and C≡C bonds characteristic of polyacetylene with

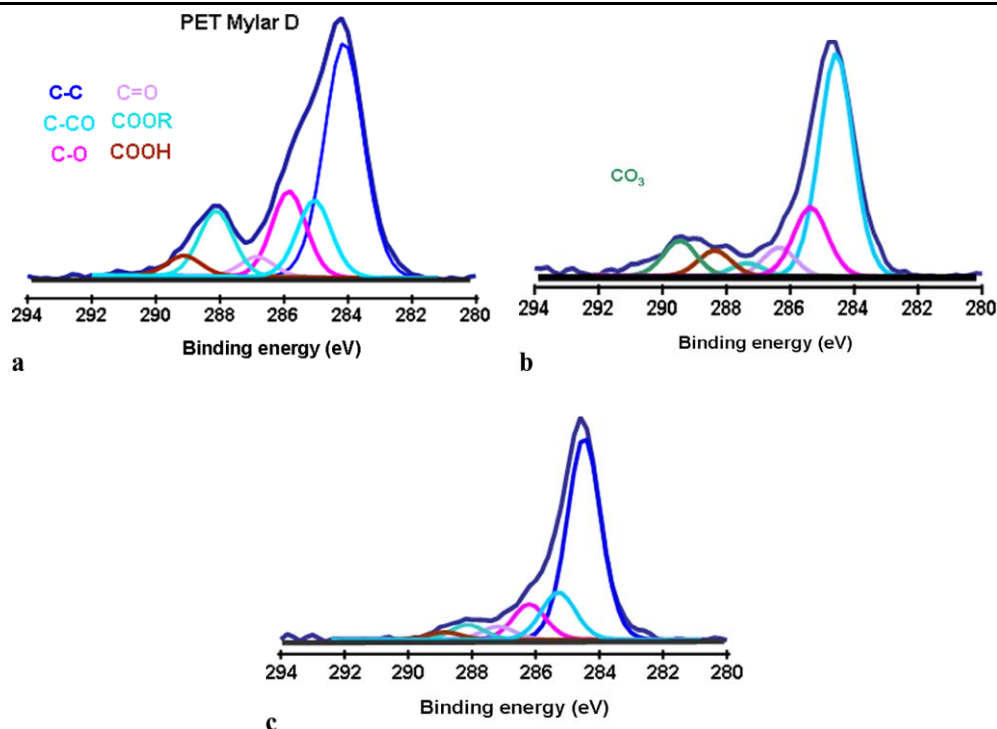


**Fig. 3** XPS spectrum of (A) virgin PET Mylar D film. XPS spectra of ablation products prepared by LA of PET: (B) at low fluence 23 mJ/cm<sup>2</sup>, 900 pulses; and (C) at high fluence 640 mJ/cm<sup>2</sup>, 40 pulses

different chain lengths along with a high density of graphitic carbon. At low fluence (26 mJ/cm<sup>2</sup>, 900 pulses), only a small density of graphitic carbon was detected.

The XPS spectrum of pristine PET Mylar D is displayed in Fig. 3(A) and is in good agreement with data previously reported [22]. It is compared to those of NP (B) and (C), the main differences are presented in Table 2. Figure 3 displays also XPS spectra of NP prepared at 23 mJ/cm<sup>2</sup> (B) and 640 mJ/cm<sup>2</sup> (C). For comparison, the main differences between XPS spectra are presented in Table 3. It appears that NP are richer in carbon than pristine PET, as indicated by the ratio C–C/C1s of samples (here C–C means carbon singly bonded to carbon and C1s is total carbon). For the high fluence case (C), the O/C ratio is reduced from 1.13 to 0.77, whereas below threshold (B), the drop of O/C is significantly less (0.92). During laser irradiation at any fluence (23, 640 mJ/cm<sup>2</sup>), the ratio COOR/C1s is reduced upon ablation which indicates that the ester group is preferentially dissociated during LA. The most striking result is the twofold increase of the ratio COOH/C1s near the ablation threshold (sample B). In order to check if there is a contribution of the substrate pollution, a drop of pure water was deposited above and was analysed by XPS under the same conditions as the previous samples B and C. The ratio of COOH/C1s was about 2.17, which is much lower than those obtained in case of B and C. This could indicate a possible hydrolysis reaction of PET in addition to photochemical degradation and

**Table 2** Data from curve fitting of spectra displayed in Fig. 3(A), (B), (C)

	C–C: 284 eV, COOR: 288 eV, COOH: 289 eV		
	A (PET)	B (NP low F)	C (NP high F)
O/C	1.13	0.92	0.77
C–C/C1s	48.9	55.3	59.7
COOR/C1s	12	5.4	4.8
COOH/C1s	2.9	5.8	3

**Table 3** Nominal height and width of NP issued from LA of different polymers and determined by statistical study of AFM images. All suspension were prepared at fluence 500 mJ/cm<sup>2</sup>, 100 except PMMA which was ablated at 1 J/cm<sup>2</sup>, 100 pulses

Polymer	Nominal height (nm)	Nominal widths (nm)
PET Mylar D	4	1–50
PEN	3	60–80
PI	2	80
PS	0.5	60–90
PMMA	4	80

therefore may explain the reduction of the ablation threshold of this polymer in water.

Similarly to PET Mylar D, underwater LA of PEN, PI, PMMA and PS allows the preparation of organic NP suspen-



sions. We obtained NP having a 3 nm in height and 80 nm in width (on average) (see Table 3). Fluence effect on PSD produced from these polymers was examined by a statistical analysis of AFM images. For this purpose, PEN, PI and PS were subjected to KrF LA in water at fluences 100 and 500 mJ/cm<sup>2</sup>. For the case of PMMA, the fluences 625 mJ/cm<sup>2</sup> and 1 J/cm<sup>2</sup> were applied; the number of pulses was fixed to 100 for all preparations. The conclusion is that height and width of NP increases with fluence in case of all polymers. This influence is small only in the case of PEN, but significantly larger for PMMA, PS and PI. These NP were also identified by CMRS. We obtained only a graphitic carbon in case of LA of PI, similar products to PET Mylar D in case of PEN, and finally, some oligomers of polystyrene and graphitic carbon were identified in case of LA of PS. Upon LA of PEN, PI and PS, graphitic carbon production could be expected because of high absorption coefficients of these polymers at laser wavelength (248 nm) [23] (see the section below). In case of PMMA which is the less absorbing, Raman spectra show formation of little graphitic carbon particles, but most of NP analysed have a spectrum which was similar to that of PMMA film revealing no great damage of this polymer during NP formation. Lazare et al. [24] highlighted PMMA nanofibers synthesis upon LA in air due to liquid expulsion that follows PMMA melting and expansion. It is possible that NP of PMMA detected here, were produced by this mechanism.

#### 4 Discussion

Briefly, it is interesting to speculate on the particular point of the ablation mechanisms leading to the formation of the nanoparticles. Two main pathways may be put forward one called “condensation” and the other “fragmentation”. In the case of carbon NP, it is thought that they form by saturated carbon vapour condensation in the plume [25] during the expansion phase after the heating phase due to absorption of the laser pulse. Condensation is, for instance, due to low vapour tension of carbon atoms, which makes even at elevated temperature, carbon particles growth possible. Therefore, it is a purely thermal pathway that follows the atomisation of the polymeric matter by the ablation process. On the other hand fragmentation is a mechanical effect due to the hydrodynamical expansion of the heated volume. It results in the breaking the material into small particles due to the rapid thermoelastic expansion and tensile stress (Model of Grandy). Therefore, it may be a low temperature pathway preserving the chemical structure of the polymer. This would explain the formation of the polymer-like NP.

#### 5 Conclusion

By KrF laser ablation of various polymers in water several types of nanoparticles were formed. Analysis by dedicated

techniques indicates that they are mainly composed of carbonaceous NP and polymer-like NP. Suspensions are rich in particles aggregates which are formed concomitantly to isolate NP. The fluence effect on PSD was examined using Mie theory and the conclusion is that increasing fluence enhances aggregation of NP. Varying the polymer structures allowed the observation of how NP populations depend on them. Possible mechanisms are either condensation or fragmentation or both.

**Acknowledgements** Regional Council of Aquitaine and CNRS (Centre National de Recherche Scientifique) of France.

#### References

1. G.W. Yang, J.B. Wang, *Appl. Phys. A* **71**, 343 (2000)
2. G.W. Yang, *Prog. Mater. Sci.* **52**, 648 (2007)
3. Y.H. Wang, R.Q. Yu, Z.Y. Liu, R.B. Huang, L.S. Zheng, X.F. Zhang, *Chem. J. Chin. Univ.* **18**, 293 (1997)
4. I. Brigger, C. Dubernet, P. Couvreur, *Adv. Drug. Deliv. Rev.* **54**, 631 (2002)
5. E. Katz, I. Willner, *Angew. Chem.* **43**, 6042 (2004)
6. X. Luo, A. Morrin, A.J. Killard, M.R. Smyth, *Electroanalysis* **18**, 319 (2006)
7. Y. Xiao, F. Patolsky, E. Katz, J.F. Hainfield, I. Willner, *Science* **299**, 1877 (2003)
8. G. Oberdörster, E. Oberdörster, J. Oberdörster, *Environ. Health Perspect.* **113**, 823 (2005)
9. G. Compagnini, A. Scalisi, O. Puglisi, *Phys. Chem. Chem. Phys.* **4**, 2787 (2002)
10. S.I. Dolgaev, A.V. Simakin, V.V. Voronov, G.A. Shafeev, F. Bozon-Verduraz, *Appl. Surf. Sci.* **186**, 546 (2002)
11. G. Compagnini, A. Scalisi, C. Spinellilla, O. Puglisi, *J. Mater. Res.* **19**, 2795 (2004)
12. T.A. Dobbins, D. Poondi, J. Singh, *J. Mater. Synth. Process.* **7**, 261 (1999)
13. D. Poondi, J. Singh, *J. Mater. Sci.* **35**, 2467 (2000)
14. J.H. Ryu, G.S. Park, K.M. Kim, C.S. Lim, J.-W. Yoon, K.B. Shim, *Appl. Phys. A* **88**, 731 (2007)
15. S. Lazare, V. Granier, *Laser Chem.* **10**, 25 (1989)
16. I. Elaboudi, S. Lazare, C. Belin, J.L. Bruneel, L. Servant, *Appl. Surf. Sci.* **253**, 7835 (2007)
17. I. Elaboudi, S. Lazare, C. Belin, J.L. Bruneel, L. Servant, *J. Phys. Conf. Ser.* (2007, in press)
18. C.F. Bohren, D.R. Huffman, *Absorption and Scattering of Light by small Particles* (Wiley, New York, 1983)
19. S.H. Hong, J. Winter, *J. Appl. Phys.* **100**, 064303 (2006)
20. S. Lazare, J.C. Soullignac, P. Fragnaud, *Appl. Phys. Lett.* **50**, 624 (1987)
21. I. Elaboudi, S. Lazare, C. Belin, D. Talaga, C. Labrugère, *Appl. Phys. A*. doi:10.1007/s00339-008-4567-2
22. S. Lazare, R. Srinivasan, *J. Phys. Chem.* **90**, 2124 (1986)
23. S. Lazare, V. Tokarev, Chap. 5, in *Laser Processing of Engineering Materials*, ed. by J. Perrière, E. Fogarassy, E. Millon. E-MRS Series (Elsevier, Amsterdam, 2006)
24. F. Weisbuch, V. Tokarev, S. Lazare, C. Belin, J.L. Bruneel, *Thin Solid Films* **453**, 394 (2004)
25. A. Kabashin, M. Meunier, Chap. 1, in *Laser Processing of Engineering Materials*, ed. by J. Perrière, E. Fogarassy, E. Millon. E-MRS Series (Elsevier, Amsterdam, 2006)